

3. Hatanaka H, Nakagawa Y. Clinical results of long surviving brain tumor patients who underwent boron neutron capture therapy. *Int J Radiat Oncol Biol Phys* 1994;28:1061-1066.
4. Farr LE, Sweet WH, Robertson JS, et al. Neutron capture therapy with boron in the treatment of glioblastoma multiforme. *Roentgenol* 1954;71:1279-1293.
5. Coderre JA, Bergland R, Chadha M, et al. Boron neutron capture of glioblastoma multiforme using p-boronophenylalanine-fructose complex and epithermal neutrons. In: Mishima Y, ed. *Cancer Neutron Capture Therapy*. New York: Plenum Press. 1996:553-561.
6. Kabalka GW, Davis M, Bendel P. Boron-11 MRI and MRS of intact animals infused with a boron neutron capture agent. *J Magn Reson Med* 1988;8:231-237.
7. Kabalka GW, Cheng CQ, Bendel P, Micca PL, Slatkin DN. In-Vivo Boron-11 MRI and MRS using (B24H22S2)4- in the rat. *J Magn Reson Imag* 1991;9:969-973.
8. Kabalka GW, Chao T, Bendel P. The role of boron MRI in boron neutron capture therapy. *J Neuro Oncol* 1997;33:153-161.
9. Bradshaw KM, Schweizer MP, Glover GH, et al. BSH distributions in the canine head and a human patient using B-11 MRI. *Magn Reson Med* 1995;34:48-56.
10. Hubner KF, King P, Gibbs WE, Partain CL, Washburn LC, Hayes RL, Holloway E. Clinical investigation with carbon-11-labeled amino acids using positron emission computerized tomography in patients with neoplastic disease. *IAWA/WHO Symposium Proceedings*, Vienna, 1981:515-529.
11. Hubner KF, Purvis JT, Mahaley SM Jr, et al. Brain tumor imaging by positron emission computed tomography using ¹¹C-labeled amino acids. *J Comput Assist Tomography* 1982;6:544-550.
12. Hubner KF, Smith GT, Thie JA, Stephens TS, Buonocore E. Dynamic positron emission tomography (PET) of brain tumors using l-aminocyclobutane[C-11]-carboxylic acid (l-[C-11]-ACBC) and a two-compartment model. *J Nucl Med* 1992;33:922.
13. Hubner KF, Thie, Hunter K, Smith GT, Bond H. Mechanism of uptake of l-[C-11]-aminocyclobutanecarboxylic acid (C-11-ACBC) by brain tumors examined by a new multiple time graphical analysis (MTGA) of image data acquired by positron emission tomography. In: Faulkner K, Carey B, Crellin A, et al., eds. *Proceedings of the 19th L.H. Gray Conference: Quantitative Imaging in Oncology*, London: British Institute of Radiology, 1996; 20-22.
14. Ishiwata K, Ido T, Mejia AA, Ichihashi M, Mishima Y. Synthesis and radiation dosimetry of 4-borono-2-[F-18]fluoro-D,L-phenylalanine: a target compound for PET and boron neutron capture therapy. *Appl Radiat Isot* 1991;42:325-328.
15. Reddy NK, Kabalka GW, Longord CPD, Roberts J, Timothy Gotsick. 4-[B-10]Borono-2-[F-18]fluoro-L-phenylalanine-fructose complex for use in timing boron neutron capture therapy (BNCT). *J Labelled Compd Radiopharm* 1995;37:599-600.
16. Smith GT, Jones RC, Hubner KF, Bond HW. A simple method to determine arterial input function data in quantitative PET [Abstract]. *Proceedings of the Radiological Society of North America 80th Scientific Assembly and Annual Meeting* 1995:326.
17. Hoffman EJ, Huang SC, Phelps ME. Quantitation in positron emission computed tomography: 1. Effect of object size. *J Comput Assist Tomography* 1979;3:299-308.
18. Imahori Y, Ueda S, Ohmori Y, et al. A basic concept for a PET-BNCT system. In: Mishima Y, ed. *Cancer neutron capture therapy*. New York: Plenum Press; 1996: 691-696.
19. Huang SC, Phelps ME, Hoffman EJ, et al. Noninvasive determination of local cerebral metabolic rate of glucose in man. *Am J Physiol* 1980;238:E69-E82.
20. Mankoff DA, Shields AF, Graham MM, Link JM, Krohn KA. A graphical analysis method to estimate blood-to-tissue transfer constants for tracers with labeled metabolites. *J Nucl Med* 1996;37:2049-2057.
21. Coderre JA, Morris GM, Micca PL, Fisher CD, Ross GM. Comparative assessment of single-dose and fractionated boron neutron capture therapy. *Radiation Research* 1995;144:310-317.
22. Barth RF, Adams DM, Soloway AH, Mechtner EB, Elam F, Anisuzzman ALM. Determination of boron in tissues and cells using direct current plasma atomic absorption emission spectroscopy. *Anal Chem* 1991;63:890-892.
23. Ishiwata K, Ido T, Kawamura M, Kubota K, Ichihashi M, Mishima Y. 4-borono-2-[F-18]fluoro-D,L-phenylalanine as a target compound for boron neutron capture therapy: tumor imaging potential with positron emission tomography. *Int J Radiat Appl Instrum B* 1991;18:745-751.
24. Ishiwata K, Shiono M, Kubota K, et al. A unique in vivo assessment of 4-[B-10]borono-L-phenylalanine in tumour tissues for boron neutron capture therapy of malignant melanomas using positron emission tomography and 4-borono-2-[F-18]fluoro-L-phenylalanine. *Melanoma Res* 1992;2:171-174.
25. Matsuda H, Oba H, Seki H, et al. Determination of flow and rate constants in a kinetic model of ^{99m}Tc-hexamethyl-propylene amine oxime in the human brain. *J Cereb Blood Flow Metab* 1988;8 (suppl):S61-S68.
26. Neirinckx RD, Burke JF, Harrison RC, Forster AM, Andersen AR, Lassen NA. The retention mechanism of technetium-99m-HMPAO: intracellular reaction with glutathione. *J Cereb Blood Flow Metab* 1988;8 (suppl):S4-S12.
27. Smith GT, Stubbs JB, Hubner KF, Goodman MM. Dynamic PET scanning and compartmental model analysis to determine cellular level radiotracer distribution in vivo. *Proceedings of the Fifth International Radiopharmaceutical Dosimetry Symposium*, Oak Ridge, TN May 1991:371-384.
28. Stubbs JB, Smith GT, Stabin MG, Eckerman KF, Turner JE. An approach to cellular level dosimetry using compartmental model analysis and dynamic PET. *Proceedings of the Fifth International Radiopharmaceutical Dosimetry Symposium*, Oak Ridge, TN May 1991:385-395.
29. Nigg DW, Eng D. Methods for radiation dose distribution analysis and treatment planning in boron neutron capture therapy. *Int J Radiation Oncology Biol Phys* 1994;28:1121-1134.
30. Kobayashi T, Kanda K. Analytical calculation of boron-10 dosage in cell nucleus for neutron capture therapy. *Radiation Research* 1982;91:77-94.

Parathyroid Hyperplasia, Thymic Carcinoid and Pituitary Adenoma Detected with Technetium-99m-MIBI in MEN Type I

Juan E. Perez-Monte, Manuel L. Brown, Martha R. Clarke, Charles G. Watson and Sally E. Carty

Departments of Radiology, Pathology and Surgery, University of Pittsburgh Medical Center, Pittsburgh, Pennsylvania

We report a case of a 57-yr-old woman with history of multiple endocrine neoplasia type I (MEN I). A ^{99m}Tc-sestamibi scan demonstrated a hyperplastic parathyroid gland, a large anterior mediastinal mass and a pituitary adenoma during a study done to evaluate recurrent hyperparathyroidism. The importance of this case is that much of the nonparathyroid pathology in patients with MEN I syndrome may be detected with this one study.

Key Words: multiple endocrine neoplasia type I; sestamibi; carcinoid; parathyroid adenoma; hyperparathyroidism

J Nucl Med 1997; 38:1767-1769

Type I multiple endocrine neoplasia (MEN I) is a hereditary autosomal dominant syndrome consisting of pituitary, parathyroid and pancreatic islet cell neoplasms (1). The clinical

expression of each of the three major components of MEN I within and among affected families is variable. Hyperparathyroidism is the most common endocrine abnormality in MEN I, and is biochemically present in 90% of patients at the time of diagnosis (2-5).

Symptoms of MEN I typically appear during the third to fifth decades, but screening laboratory tests for asymptomatic hypercalcemia may identify affected individuals at an earlier age (4,6). The spectrum of symptoms and signs of hyperparathyroidism in MEN I is similar to that observed in sporadic primary hyperparathyroidism. The common clinical manifestations include urolithiasis, peptic ulcer disease, emotional lability and bone pain. Multiple parathyroid gland hyperplasia is the characteristic finding in MEN I related hyperparathyroidism (5).

CASE REPORT

The case of a 57-yr-old woman with MEN I is presented. The patient's brother has hyperparathyroidism and a gastrinoma, and

Received Oct. 9, 1996; revision accepted Feb. 19, 1997.

For correspondence, contact: Manuel L. Brown, MD, Department of Radiology, University of Pittsburgh Medical Center, 200 Lothrop St., Pittsburgh, PA 15213.

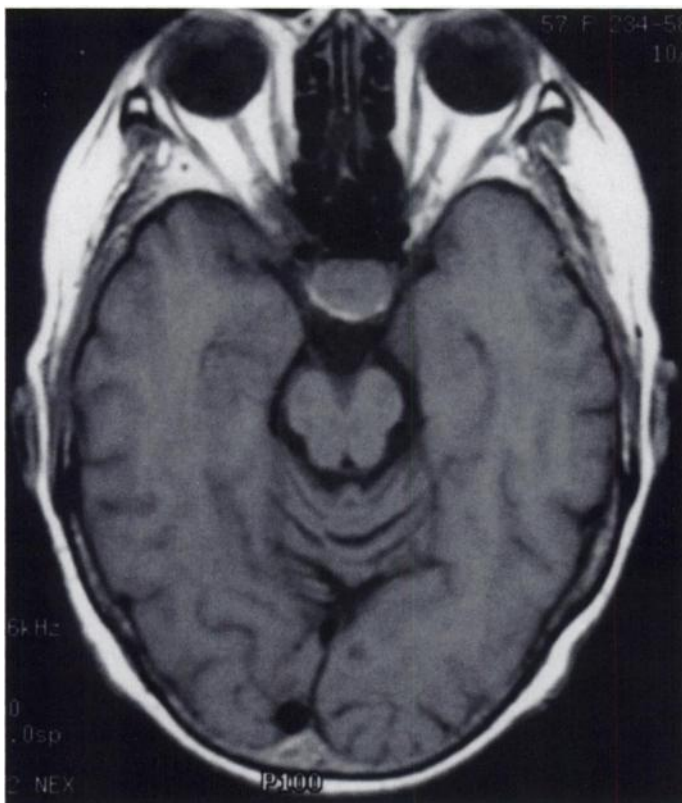


FIGURE 1. MRI transaxial image showing a 1.5 × 2.0 cm suprasellar mass consistent with a pituitary prolactinoma.

her mother died of the Zollinger-Ellison syndrome. The patient's history is characterized by the following: (1) hyperprolactinemia with a 2 cm clinically silent alpha subunit secreting pituitary adenoma detected prospectively by MRI in 1993 (Fig. 1); (2) hyperparathyroidism treated in February 1971 by subtotal parathyroidectomy and in May 1994 by excision of fifth and sixth (supranumary) neck glands; and (3) a 2-cm pancreatic islet cell lesion treated by excision.

In May 1995, a ^{99m}Tc -sestamibi SPECT scan was performed in an attempt to locate additional parathyroid tissue that was suggested by recurrent biochemical hyperparathyroidism. This study detected an area suspicious for an ectopic parathyroid gland in the thoracic inlet on the right side (Fig. 2A). The known pituitary adenoma was also imaged by the sestamibi (Fig. 2B). One month prior, a large anterior mediastinal mass had been detected on a

FIGURE 2. (A) Anterior reprojection image of a SPECT ^{99m}Tc -sestamibi scan localizing a right thoracic inlet hyperplastic parathyroid gland in the submanubrial region (arrow). In addition, a large diffuse irregular mass, with less intense uptake in the anterior mediastinum, was found to be a thymic carcinoid tumor (arrow-heads). (B) Transaxial slice of the head showing the increased tracer activity in the pituitary adenoma.

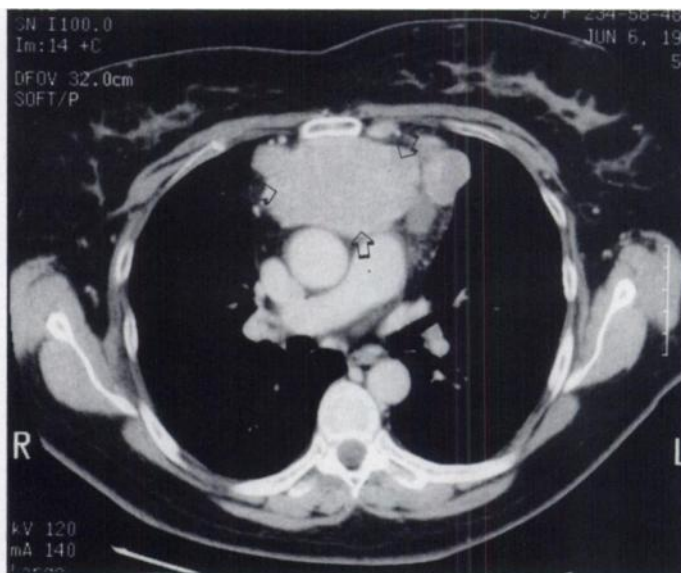
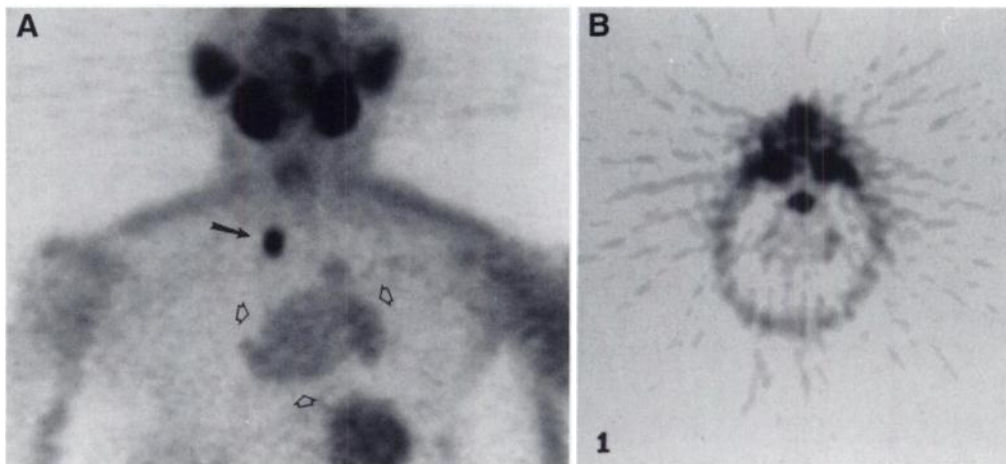


FIGURE 3. CT of the chest shows the sharply margined and lobulated anterior mediastinal mass (arrows) measuring 4.5 × 3.5 cm originating from the thymic bed; fine-needle aspiration demonstrated a thymic carcinoid tumor.

chest radiograph and evaluated by a CT (Fig. 3). The mass also was seen on the sestamibi images (Fig. 2A). Ultrasound guided biopsy of the anterior mediastinal mass yielded tissue consistent with a thymic carcinoid tumor. A malignant thymic carcinoid tumor was resected in June 1995 along with a 97-mg parathyroid gland. The patient's abdomen was not imaged with the sestamibi, and, therefore, we do not know if the pancreatic tumor would have been tracer avid.

Pathology

The mediastinal mass was resected with an adjacent 2-cm portion of left upper lobe of lung and a 7.5 × 5.0 × 0.2-cm portion of pericardium. The tumor measured 11 × 7.2 × 3.0 cm and had a distinct lobular, tan appearance with focal hemorrhage, cystic degeneration and calcification. A separate, 3 × 2.5 × 1.5-cm tumor nodule was removed from the left superior thymic extension. Grossly normal appearing fatty thymic tissue was also submitted. Approximately one-third of an enlarged, ectopic supernumerary right inferior parathyroid gland was submitted that weighed 97 mg and measured 8 × 7 × 7 mm. The remaining portions were cryopreserved and one part implanted into the left brachioradialis muscle.

Histologically, the thymic carcinoid tumor was composed of relatively uniform round to spindle shaped cells with pale eosinophilic cytoplasm in a solid growth pattern. Mild nuclear atypia

was present and mitotic figures were identified. The tumor cells were positive for neuron specific enolase, synaptophysin and cytokeratin AE1/AE3 and negative for chromogranin and ACTH. Vascular invasion was present, as well as extension beyond the capsule into the adjacent adipose tissue. Microscopic foci of tumor was present in the grossly normal appearing thymus and metastatic tumor was present in one of four lymph nodes.

The parathyroid gland was hypercellular with a diffuse proliferation of chief cells and oxyphil cells, which is consistent with hyperplasia. A microscopic focus of metastatic carcinoid tumor was present within the parathyroid gland.

The enucleated pancreatic endocrine tumor measured 2.5 cm in greatest dimension and was resected with a small rim of uninvolved pancreatic tissue. The tumor was white-tan in color and showed cystic degeneration. Histologically, the tumor was composed of nests and trabeculae of neuroendocrine cells typical of islet cell tumor. Immunohistochemical stain for chromogranin was positive in the tumor cells and somatostatin was weakly positive in a focal distribution. Glucagon and insulin were negative. The small portion of adjacent pancreatic parenchyma showed no evidence of islet cell hyperplasia.

DISCUSSION

Thymic carcinoid tumors are rare in both the sporadic and MEN setting. In both instances, the clinical features, including a high incidence of Cushing's syndrome and frequent presentation at an advanced stage are similar (8). Surgical extirpation is the therapy of choice and adjuvant chemotherapy and radiation therapy do not appear to confer a survival benefit (8,9). Given the high rate of metastases and tumor-related deaths associated with these tumors, screening for these neoplasms seems warranted, especially in patients with MEN I who may be undergoing evaluation for hyperparathyroidism. This has been recommended by other authors who have documented an 88% rate of concomitant hyperparathyroidism in MEN patients with thymic carcinoid, and 39% rate of thymic carcinoid in MEN patients with hyperparathyroidism (10).

The association of carcinoid tumors with MEN I was first reported by Underdahl in 1953 (6). Since then, more than 50 cases of carcinoid tumor associated with other endocrine tumors have been reported. Carcinoid tumors occur in 5%–9% of patients with MEN I. The most frequent sites of origin are the bronchus, duodenum and thymus.

Technetium-99m-sestamibi (Cardiolite) was originally developed for myocardial perfusion studies as an alternative to ^{201}Tl chloride (7,11). It is a monovalent cation complex with a central Tc(I) core octahedrally surrounded by six identical alkyl isonitrile groups that are coordinated through the isonitrile carbon. The surrounding terminal alkyl groups give the complex a moderate lipophilic property (12). Technetium-99m-sestamibi uptake in tumors is proportional to blood flow (13). Its uptake mechanism involves passive diffusion across plasma and mitochondrial membranes. At equilibrium, strong negative transmembrane potentials propagate a concentration of the agent within the inner matrix of mitochondria (12,14). Since the early 1990s, an increasing number of articles have been published describing uptake of $^{99\text{m}}\text{Tc}$ -sestamibi in tumors. Case reports describing uptake in breast carcinoma (15), osteosarcoma (16), bronchogenic carcinoma (17) and parathyroid carcinoma (18), as well as in medullary thyroid carcinoma (19) have been reported. The augmented uptake in malignant tumors is believed to be caused by stronger negative mitochondrial and plasma membrane potentials secondary to increased metabo-

lism of tumor cells (12,20). Indirect mechanisms, such as an increase of blood flow and capillary permeability, have also been suggested (21). Technetium-99m-sestamibi is also accumulated in benign tumors and it is used for detection and localization of parathyroid adenomata (22–24).

CONCLUSION

The parathyroid hyperplasia, thymic carcinoid tumor and pituitary adenoma in the case reported were all detected by $^{99\text{m}}\text{Tc}$ -sestamibi. Technetium-99m-sestamibi has become the standard imaging modality for localization of parathyroid adenomas. Its accumulation is nonspecific and, because of this, as demonstrated in the case report, examination with this agent can potentially localize nonparathyroid endocrine pathology in patients with the MEN I syndrome, complementary with imaging studies.

REFERENCES

1. Gagel RF. Multiple endocrine neoplasia. In: Wilson J, Foster D. *Williams textbook of endocrinology*, 8th ed. Philadelphia, PA: Saunders 1992;1537–1553.
2. Skogseid B, Eriksson B, Lundquist G, et al. Multiple endocrine neoplasia Type I: a 10-year prospective screening study in four kindreds. *J Clin Endocrinol Metab* 1991;73:281–287.
3. Van Heerden JA, Kent RB III, Sizemore GW, Grant CS, ReMine WH. Primary hyperparathyroidism in patients with multiple endocrine neoplasia syndromes. *Arch Surg* 1983;118:533–536.
4. Leshin M. Multiple endocrine neoplasia. In: Wilson J, Foster D, eds. *Williams textbook of endocrinology*, 7th ed. Philadelphia, PA: Saunders 1989;1274–1290.
5. Benson L, Ljunghall S, Akerstrom G, Oberg K. Hyperparathyroidism presenting as the first lesion in multiple endocrine neoplasia type I. *Am J Med* 1987;82:731–737.
6. Underdahl LO, Woolner LB, Black BM. Multiple endocrine adenomas. report of 8 cases in which the parathyroids, pituitary and pancreatic islets were involved. *J Clin Endocrinol Metab* 1953;13:20–47.
7. Holman BL, Jones AG, Lister-James J, et al. A new Tc-99m-labeled myocardial imaging agent, hexakis (t-butylisonitrile)-technetium(I) [$^{99\text{m}}\text{Tc}$], Initial experience in the human. *J Nucl Med* 1984;25:1350–1355.
8. Zeiger MA, Swartz SE, MacGillivray DC, Linnoila I, Shakir M. Thymic carcinoid in association with MEN syndromes. *Am Surg* 1992;58:430–434.
9. Asbun HJ, Calabria PP, Calmes S, Lang AG, Bloch JH. Thymic carcinoid. *Am Surg* 1991;57:442–445.
10. Duh Q-Y, Hybarger CP, Geist R, et al. Carcinoid associated with multiple endocrine neoplasia syndromes. *Am J Surg* 1987;154:142–148.
11. Wackers FJT, Berman DS, Maddahi J, et al. Technetium-99m hexakis 2-methoxyisobutyl isonitrile: human biodistribution, dosimetry, safety, and preliminary comparison to thallium-201 for myocardial perfusion imaging. *J Nucl Med* 1990;31:1646–1653.
12. Chiu ML, Kronauge JF, Piwnicka-Worms D. Effect of mitochondrial and plasma membrane potentials on accumulation of hexakis (2-methoxy-isobutylisonitrile) technetium (I) in cultured mouse fibroblasts. *J Nucl Med* 1990;31:1646–1653.
13. Beller GA, Watson DD. Physiological basis of myocardial perfusion imaging with the technetium 99m agents. *Semin Nucl Med* 1991;21:173–181.
14. Delmon-Moingeon LI, Piwnicka-Worms D, Van den Abbeele AD, et al. Uptake of the cation hexakis(2-methoxyisobutylisonitrile)-technetium-99m by human carcinoma cell lines in vitro. *Cancer Res* 1990;50:2198–2202.
15. Campeau RJ, Kronemer KA, Sutherland CM. Concordant uptake of Tc-99m sestamibi and Tl-201 in unsuspected breast tumor. *Clin Nucl Med* 1992;17:936–937.
16. Caner B, Kitapci M, Aras T, et al. Increased accumulation of hexakis (2-methoxyisobutylisonitrile) technetium(I) in osteosarcoma and its metastatic lymph nodes. *J Nucl Med* 1991;32:1977–1978.
17. Strouse PJ, Wang DC. Incidental detection of bronchogenic carcinoma during Tc-99m sestamibi cardiac imaging. *Clin Nucl Med* 1993;18:448–449.
18. Kitapci MT, Tastekin G, Turgut M, et al. Preoperative localization of parathyroid carcinoma using Tc-99m MIBI. *Clin Nucl Med* 1993;18:217–218.
19. O'Driscoll CM, Baker F, Casey MJ, et al. Localization of recurrent medullary thyroid carcinoma with technetium-99m-methoxyisobutylisonitrile scintigraphy: a case report. *J Nucl Med* 1991;32:2281–2283.
20. Chen LB. Mitochondrial membrane potentials in living cells. *Ann Rev Cell Biol* 1988;4:155–181.
21. Aktolun C, Bayhan H, Kir M. Clinical experience with Tc-99m MIBI imaging in patients with malignant tumors. Preliminary results and comparison with Tl-201. *Clin Nucl Med* 1992;17:171–176.
22. Coakley AJ, Kettle AG, Wells CP, O'Doherty MJ, Collins REC. Tc-99m sestamibi-a new agent for parathyroid imaging. *Nucl Med Commun* 1989;10:791–794.
23. O'Doherty MJ, Kettle AG, Wells T, et al. Parathyroid imaging with technetium 99m-sestamibi: preoperative localization and tissue uptake studies. *J Nucl Med* 1992;33:313–318.
24. Taillefer R, Boucher Y, Potvin C, et al. Detection and localization of parathyroid adenomas in patients with hyperparathyroidism using a single radionuclide imaging procedure with technetium-99m sestamibi (double phase study). *J Nucl Med* 1992;33:1801–1807.